

**Final Report**

**Interagency Memorandum of Understanding  
Among The NEXRAD Program,  
The WSR-88D Radar Operations Center,  
The NWS Office of Hydrologic Development**

**June 1, 2002 to May 31, 2003**

**Feng Ding  
Dong-Jun Seo  
Richard Fulton  
David Kitzmiller**

**Hydrology Laboratory  
Office of Hydrologic Development  
NOAA National Weather Service**

**November 17, 2003**

## Table of Contents

- 1. Validation of Range Correction Algorithm Using Real-time Radar Data from Sterling, VA**
  - 1.1 Introduction
  - 1.2 Data Set
  - 1.3 Evaluation Results
    - 1.3.1 Radar-Only Evaluation
    - 1.3.2 Gauge-Radar Evaluation
  - 1.4 Conclusions
  - References
  
- 2. Convective-Stratiform Separation Algorithm (CSSA) Development and Evaluation**
  - 2.1 Introduction
  - 2.2 Description of the full CSSA
  - 2.3 Estimation of Indicator Statistics
  - 2.4 Evaluation and Results
    - 2.4.1 KDDC (Dodge City, KS)
    - 2.4.2 KEVX (Eglin AFB, FL)
    - 2.4.3 KFDR (Frederick, OK)
    - 2.4.4 KHGX (Houston, TX)
    - 2.4.5 KINX (Tulsa, OK)
    - 2.4.6 KMLB (Melbourne, FL)
    - 2.4.7 KOKX (Brookhaven, NY)
  - 2.5 Summary, Conclusions and Recommendations
  - References
  
- 3. Development and Analysis of WSR-88D Hydrometeorological Algorithms**  
Princeton University
  
- 4. Vertical Profile of Reflectivity and Beam Occultation Studies For Improved Radar-Rainfall Estimation**  
University of Iowa
  
- 5. Appendix: Truncation Errors in Historical WSR-88D Rainfall Products**

# **1. Validation of Range Correction Algorithm Using Real-time Radar Data from Sterling, VA**

## **1.1 Introduction**

The Range Correction Algorithm (RCA) is a procedure developed by the National Weather Service (NWS) Office of Hydrological Development (OHD) Hydrology Laboratory (HL) for real-time adjustment of range-dependent reflectivity biases in Weather Surveillance Radar-1998 Doppler version (WSR-88D). The RCA corrects biases that are due to nonuniform vertical profile of reflectivity (VPR) (Seo et al. 2000), one of the most important sources of error in WSR-88D rainfall estimates (Fulton et al. 1998). The RCA is currently under implementation in the Open Radar Product Generation (ORPG) system in OHD. The prototype RCA has been running since early 2003 for validation using real-time radar data from Sterling, VA (KLWX).

In this work, we have compared the original and range-corrected DPA estimates to raingauge values to verify the performance of RCA in real-time operations, and to develop guidance for the usage of RCA. This long-duration and extensive validation is a necessary supplement to the individual case studies performed in Seo et al. (2000).

## **1.2 Data Set**

The main product of the prototype RCA is the Adjustment Factor Array (AFA). It specifies the multiplicative adjustment factors to the radar rainfall within the  $131 \times 131$  subsection of the Hydrologic Rainfall Analysis Project (HRAP) grid surrounding the radar site. These factors are used to adjust the radar rainfall estimates in the hourly Digital Precipitation Array (DPA) product. Here, we compare the original DPA and the DPA with RCA adjustment to evaluate the RCA performance.

The prototype RCA has been running in HL since early 2003, and DPA, AFA, and other RCA products have been being archived. The archival period covers most of February, March, April, and May of 2003, though data gaps exist due to radar and local workstation outage. DPA at the top of hour and the corresponding AFA are used to generate hourly radar rainfall estimates with RCA adjustment. Table 1 lists the number of DPAs at the top of hour with precipitation (rain or snow) for this study in February, March, April, and May of 2003. It also lists the number of days for which the DPAs are available. Over the four-month period, there are 1389 hours of DPA with precipitation (rain or snow), of which 217 hours are from February, 282 hours from March, 350 hours from April (Data in April 29 and 30 have serious Anomalous Propagation (AP) contamination and are excluded) and 509 hours from May.

For the comparison with rain gauge observations, we used the 24-h precipitation data ending at 12Z UTC from the National Centers for Environmental Prediction (NCEP). Those rain gauges identified as “suspect,” based on automated consistency checks, are excluded from this

analysis. The 24-h precipitation estimates from the radar are simply the summation of hourly DPAs from 13Z UTC to the following 12Z UTC. Both the original and RCA-adjusted 24-h radar precipitation estimates are compared with the gauge data. From the location of the gauge, the position of the matching HRAP grid can be obtained. A gauge-radar data pair is then defined as the 24-h precipitation amounts from the gauge and radar at the matching HRAP grid. Table 2 lists the number of gauge-radar pairs and the number of 24-h accumulations of these gauge-radar pairs available for each month. Note that, in each month, there are more than one thousand gauge-radar pairs.

Table 1. The number of DPAs with precipitation (rain or snow) and the number of days for which DPAs are available in each month of the analysis period.

Month	February	March	April*	May
Hours of DPA	217	282	350	509
Days	17	24	26	31

\*For two days in April, radar data have serious AP contamination. The numbers shown do not include these two days.

Table 2. The number of gauge-radar pairs and the number of 24-h periods for which the pairs are available in each month of the analysis period.

Month	February	March	April*	May
Gauge-radar pairs	1206	2030	1556	3483
24-h periods	12	20	14	22

\*See Table 1 note

### 1.3 Evaluation Results

#### 1.3.1 Radar-Only Evaluation

Figures 1(a) and 1(b) show the radar precipitation accumulations from all 217 hours' worth of original and RCA-adjusted DPAs in February, respectively. The range circle in the figures indicates a radius of 230 km from the radar site. Without RCA adjustment, the bright band effect is readily visible within range band between 70 and 150 km, particularly in the east and southeast part of the radar umbrella. After RCA adjustment, the bright band effects are significantly reduced, except in some areas adjacent to the terrain blockage in the southwest part of radar umbrella. Accounting for the effect of terrain blockage is not within the scope of this study and is not discussed further. It may also be seen that, with RCA adjustment, the precipitation estimates in the areas near the edge the radar umbrella are increased.

The effects of RCA adjustment are more evident in Fig. 1(c), which shows the difference

in precipitation accumulation between the RCA-adjusted and unadjusted estimates. Nonzero differences appear in three concentric bands. Near the radar site is a white circular area with radius of about 40 km. In this area, little or no adjustment was made by RCA. Beyond the white circular area is a concentric band within ranges of about 40 km to 150 km. In this zone, the mix of blue, green, and black colors indicate significant reduction in precipitation estimates brought by RCA adjustment. The maximum amount of reduction is about 25 mm. The exception is the small pink areas in the southwestern part where the second elevation angle is used for precipitation estimation due to beam blockage. In the far-range area is another concentric band with a mix of white, yellow, red and pink colors. In this area, RCA adjustment increases precipitation estimates. The maximum increase is about 55 mm over the entire month.

As noted in the Introduction, the main purpose of RCA is to reduce the range-dependent bias. To view such effect of RCA adjustment, the azimuthal averages of precipitation accumulation of the original (red dash line) and the RCA-adjusted (blue solid line) are shown in Fig. 1(d). Note in Fig. 1(d) that the three ranges of no, negative and positive adjustment correspond to the three annuli in the Fig. 1(c). The first is the close range with slant ranges less than 40 km. Over this range, RCA brings almost no adjustment. The second is the mid-range with slant ranges from about 40 km to 150 km. In this range, the azimuthal-mean precipitation with RCA adjustment is consistently smaller than that without adjustment, the result of RCA adjustment of the bright-band effect. The third is the far-range with slant ranges greater than 150 km. Over this range, the azimuthal-mean precipitation with RCA adjustment is consistently greater than that without adjustment, the result of RCA adjustment of radar sampling of frozen hydrometeor above the melting layer. While the RCA adjustment in the far-range is not as pronounced as that in the mid-range, it is apparent that the range effects are indeed mitigated at all ranges.

Figures 2 and 3 are analogous to Fig. 1, but for March and May, respectively. The result for April has a different set of issues and will be discussed later. The patterns and situations shown in Figures 2 and 3 are similar to Fig. 1, and similar conclusions may be drawn for March and May. It is worth noting that the magnitude of adjustment to precipitation amounts brought by RCA are more significant in March and May than in February, a point that may not be evident in comparison of Figures 2(d) and 3(d) to Fig. 1(d). This larger adjustment is more pronounced in the mid-range than in the far-range. For example, in February the maximum difference in the azimuthal average between the original and the RCA-adjusted is about 10 mm, whereas in March and May it is about 20 mm and 60 mm, respectively. It suggests that bright-band enhancement in March and May may have been more intense. This temporal variation in magnitude of adjustment is a reflection of different precipitation types in the three-month period. In February much of the precipitation reached the ground as snow, implying that the melting level was below or very near the surface. During March roughly half of the precipitation was rain, and virtually all precipitation was rain during May.

Figure 4 shows the anomalous results of RCA adjustment for April, when all precipitation cases were included in the sample. In Fig. 4(b), there are small areas and spots with very larger precipitation in the circular band within the slant ranges of 40 to 150 km, typically an

area where raw precipitation estimates are reduced by RCA. Such results appear as pink areas and spots in Fig. 4(c) and sharp peaks in Fig. 4(d). Examination of the reflectivity fields indicated that this unexpected result is due to very serious anomalous propagation (AP) contamination on April 29 and 30. Fig. 5 shows the results after the radar data in these two days are excluded. The results are similar to those from other months.

### 1.3.2 Gauge-Radar Evaluation

Figures 6, 7, 8, and 9 show the gauge-vs.-radar scatter-plots of 24-h precipitation for February, March, April, and May, respectively. Each figure has four panels showing the original (top-left), with mean-bias adjustment (top-right), with RCA adjustment (bottom-left), and with both mean-field bias and RCA adjustment (bottom-right). The reason for the mean-bias adjustment is that radar rainfall estimates are subject to a number of other (than the VPR effects) sources of error, which, if unaccounted for in some way, may mask the effects of RCA and hence defeat the purpose of gauge-radar evaluation. Another reason for the mean-field bias adjustment is that the Precipitation Pre-processing System (PPS) in current ORPG system has the mean-field bias adjustment functionality. Here, mean-field bias is defined as the average of the ratios of gauge-to-radar rainfall of all gauge-radar pairs in each 24-h period (note that this is different from the definition of the operationally produced estimates of mean-field bias). In each figure, different symbols are used to represent gauge-radar pairs from different slant ranges. “Blue cross” is from the near-range (less than 70km), “red star” from the mid-range (70 km to 140 km), and “green circle” from the far-range (greater than 140 km).

Figures 6 and 7 show quite similar results for February and March. In these two months, radar significantly underestimated precipitation (see the left panels). Note that, even though the mean-bias adjustment corrects the overall underestimation, RCA-unadjusted estimates have a very large scatter (see the top-right panels). RCA-adjusted estimates, on the other hand, have a significantly reduced scatter (see the bottom-right panels).

The situation in April (see Fig. 8) is somewhat different from February and March. Radar still underestimates precipitation (see the left panels) but not as severely as in February and March. However, the radar rainfall estimates have a larger scatter (see the left panels) when compared to those in February and March. It is suspected that AP contamination may have been a contributing factor. Even though the two days with serious AP contamination are excluded, there may have been other days with less severe, but still significant, AP contamination. Nevertheless, the RCA adjustment still reduces the scatter significantly (see the lower-right panel).

Fig. 9 shows the result for May. Because much of the precipitation was convective, underestimation at long ranges is no longer the dominant feature of the unadjusted-radar scatter plots (see the left panels). As shown in the right panels that, even in this largely convective month, the improvement by RCA is evident.

The statistical results including linear correlation coefficient (CC), root mean square error

(RSME), and their improvements are listed in Tables 3 and 4. The margin of improvement, shown in brackets, is with respect to the CC and RMSE of the original DPA, and quantifies the improvement brought by RCA adjustment. In Table 3, CC values with RCA adjustment are always greater than those before RCA adjustment. The improvement in CC is over 10% in all months except May. This is similar to the result (10%) of 46-h storm total precipitation of KRTX case (Portland, Oregon) in Seo. et al. (2000). For April, as noted above, the relatively poor quality of radar data (due to AP contamination) decreased the CC to rather small values. Even after the RCA adjustment, CC is only 0.39. As such, the improvement of 25.5% may not be taken seriously. In May, the improvement of RCA adjustment is smaller (only 7.5%) due to convective precipitation. Note that the prototype RCA algorithm is developed for stratiform rain events (Seo et al., 2000). To handle embedded convection, RCA will be supported by the Convective-Stratiform Separation Algorithm (CSSA) in operational implementation, which is currently under development (Seo et al. 2002, this report).

The RMSE values in Table 4 also indicate that RCA adjustment yields consistently smaller errors in 24-h precipitation. The degradation in RCA performance for convective rain events is also reflected in the RSME values

Table 3. Liner correlation coefficient (CC) values and their improvements based on the original DAP (number in the bracket) in each month.

Month	CC value and improvement ( %)	
	Original	RCA-adjusted
February	0.65	0.76 (17.6%)
March	0.71	0.80 (12.2%)
April	0.31	0.39 (25.5%)
May	0.60	0.65 (7.5%)

Table 4. Root-mean squared error (RMSE) values and their improvements based on the original DAP (number in the bracket) in each month. MB-adjusted represents with mean-bias (MB) adjustment.

Month	RMSE value (mm) and improvement ( %)			
	Original	MB-adjusted	RCA-adjusted	MB & RCA-adjusted
February	10.67	12.1 (-13.8%)	9.9 (6.9%)	9.6 (10.3%)
March	9.94	9.94 (-3.7%)	9.6 (3.0%)	8.3 (16.4%)
April	9.03	8.9 (1.3%)	8.7 (3.4%)	7.5 (16.5%)
May	9.83	11.7 (-18.7%)	9.2 (6.4%)	9.7 (1.1%)

## 1.4 Conclusions

A four-month validation using KLWX real-time data (Feb through May of 2003) indicates that the RCA algorithm consistently improves radar rainfall estimates. It is noted here that, over the validation period, the prototype RCA was under development and minor changes were made to the code and to the adaptable parameters. Even under this less-than-preferable setup, the improvement is significant in both radar-only evaluation and gauge-radar evaluation. Gauge-radar evaluation shows that the improvement in 24-h precipitation is more than 10% under the correlation coefficient and root mean square error criteria.

It was found that two factors affect the performance of the prototype RCA most significantly; the quality of radar reflectivity data (AP contamination in particular) and embedded convection. With respect to data quality, the expectation is that the implementation of the Enhanced Pre-processing (EPRE) algorithm and the Radar Echo Classifier (REC) algorithm will provide RCA with consistently high-quality reflectivity data. With respect to convection, the prototype Convective-Stratiform Separation Algorithm (CSSA, Seo et al. 2002, this report) should be matured and implemented to support RCA under the ‘stratify-and-adjust’ strategy.

## References

- Fulton, R. A., J. P. Breidenbach, D.-J. Seo, D. A. Miller, and T. O’Bannon, 1998: The WSR-88D rainfall algorithm. *Wea. Forecasting*, **13**, 377-395
- Seo, D.-J., J. P. Breidenbach, R. A. Fulton, D. A. Miller, and T. O’Bannon, 2000: Real-time adjustment of range-dependent biases in WSR-88D rainfall estimates due to nonuniform vertical profile of reflectivity. *J. Hydrometeor.*, **1**, 222-240
- Seo, D.-J. and coauthors, 2002: Final Report, Interagency Memorandum of Understanding among the NEXRAD Program, WSR-88D Operational Support Facility, and the NWS Office of Hydrologic Development.  
[Available at: [http://www.nws.noaa.gov/ohd/hrl/papers/2002mou/Mou02\\_PDF.html](http://www.nws.noaa.gov/ohd/hrl/papers/2002mou/Mou02_PDF.html)]

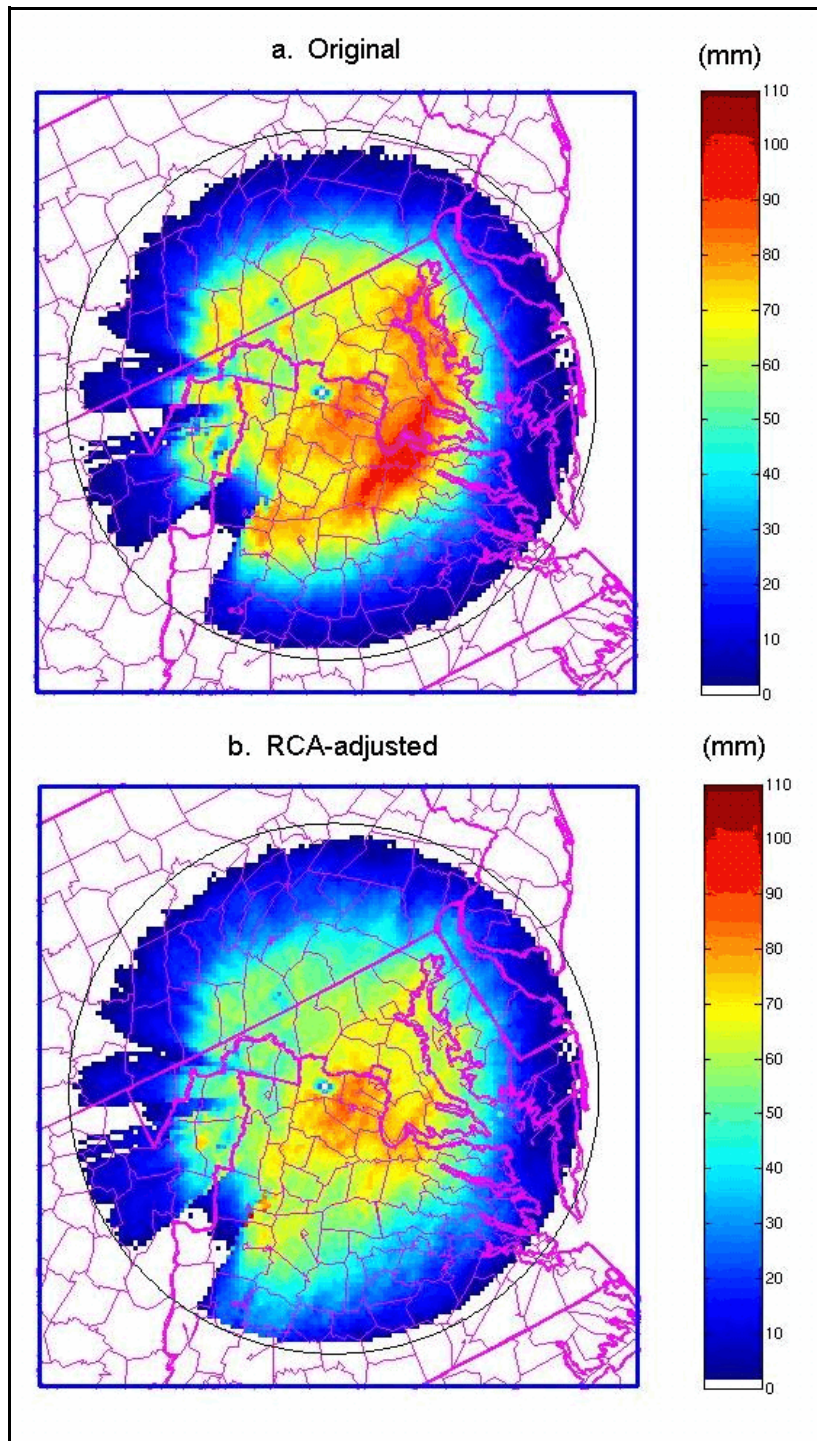


Figure 1. Radar precipitation accumulations from (a) the original DPA, and (b) DPA with RCA adjustment, in February 2003.

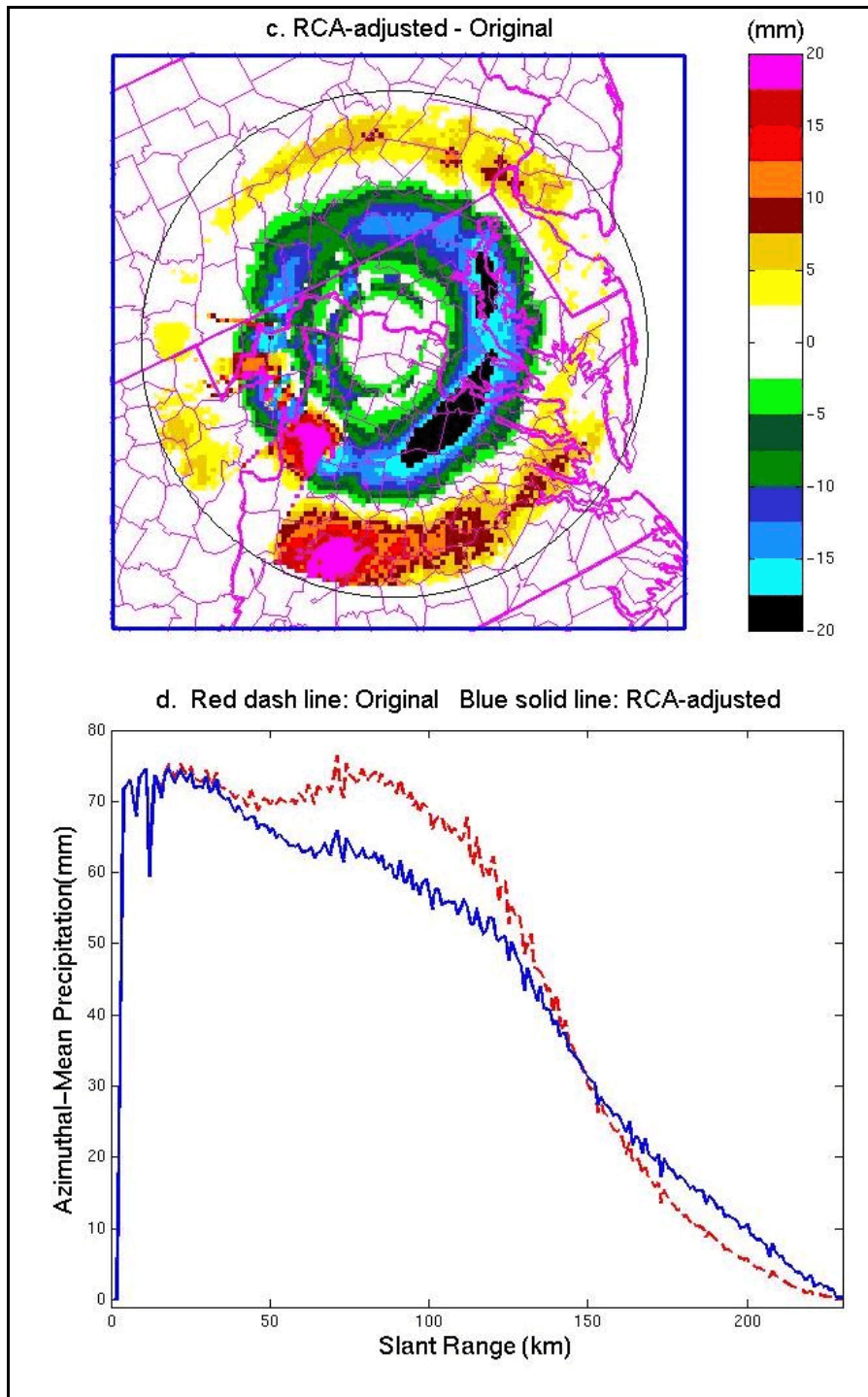


Figure 1(continued). (c) Difference of precipitation accumulations between the original and with RCA adjustment, and (d) Azimuthal averages of precipitation accumulations from the original (red dash line) and with RCA adjustment (blue solid line), in February 2003.

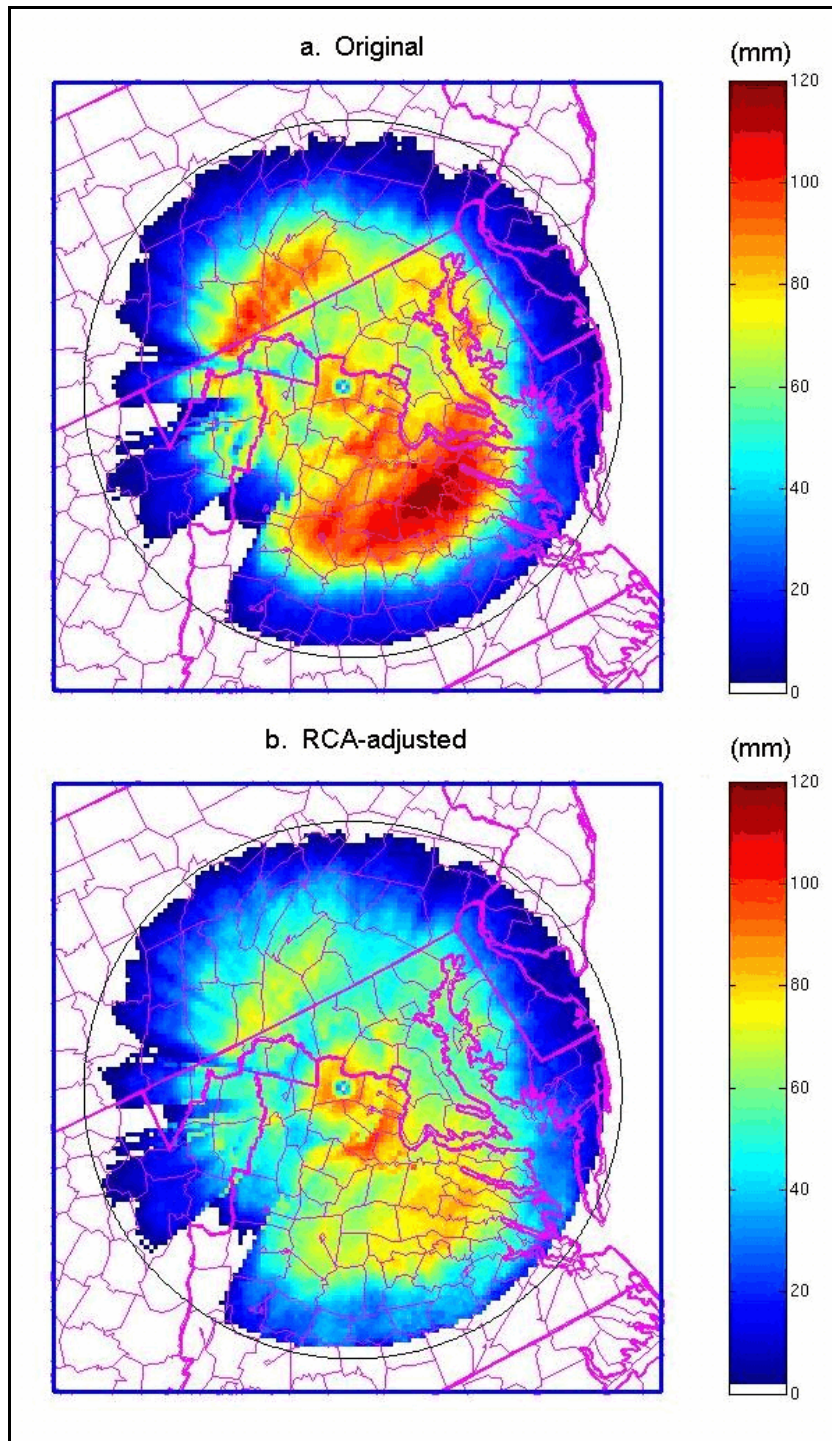


Figure 2. As in Fig. 1a,b but for March 2003.

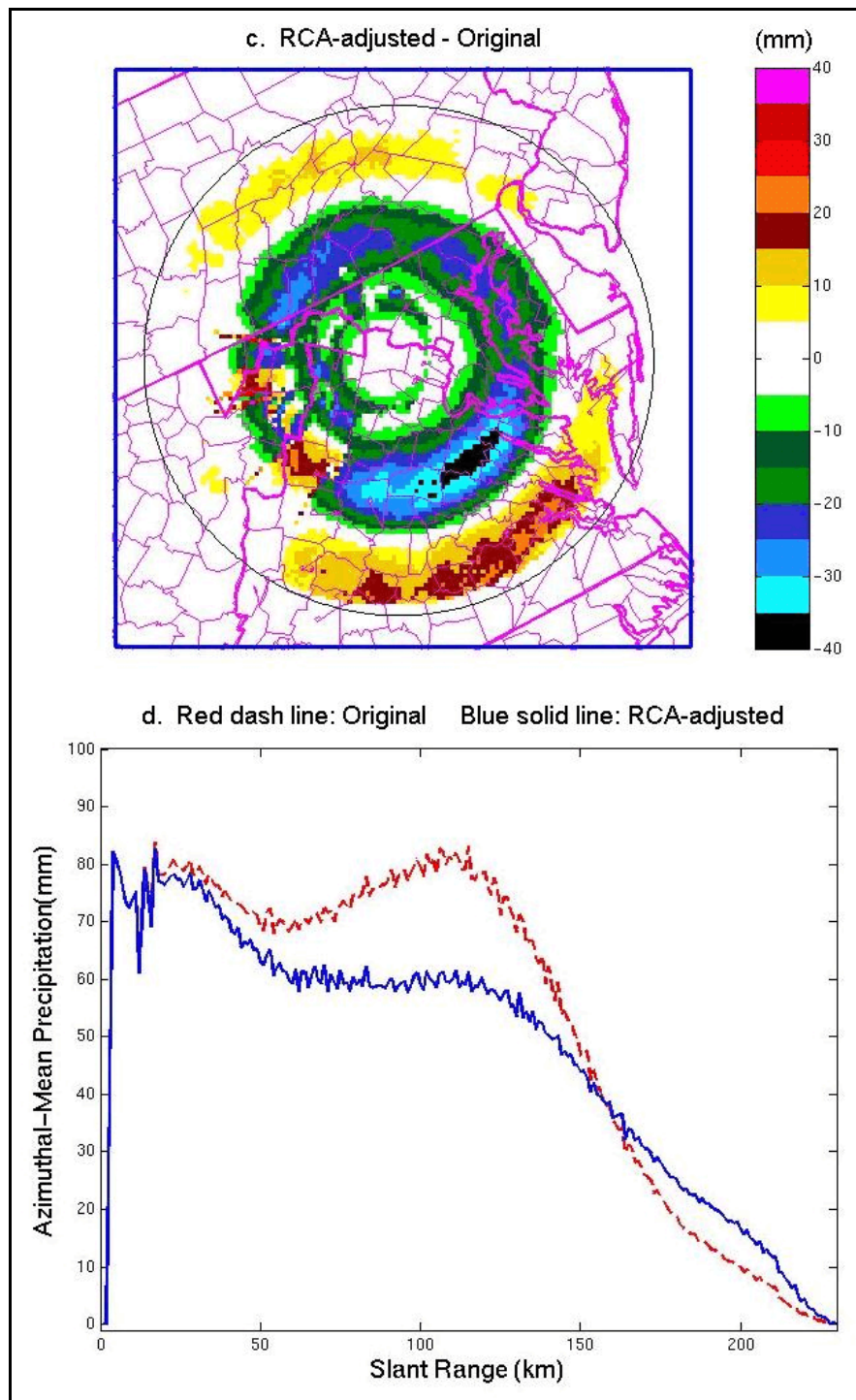


Figure 2(continued). As in Fig. 1c,d but for March 2003.

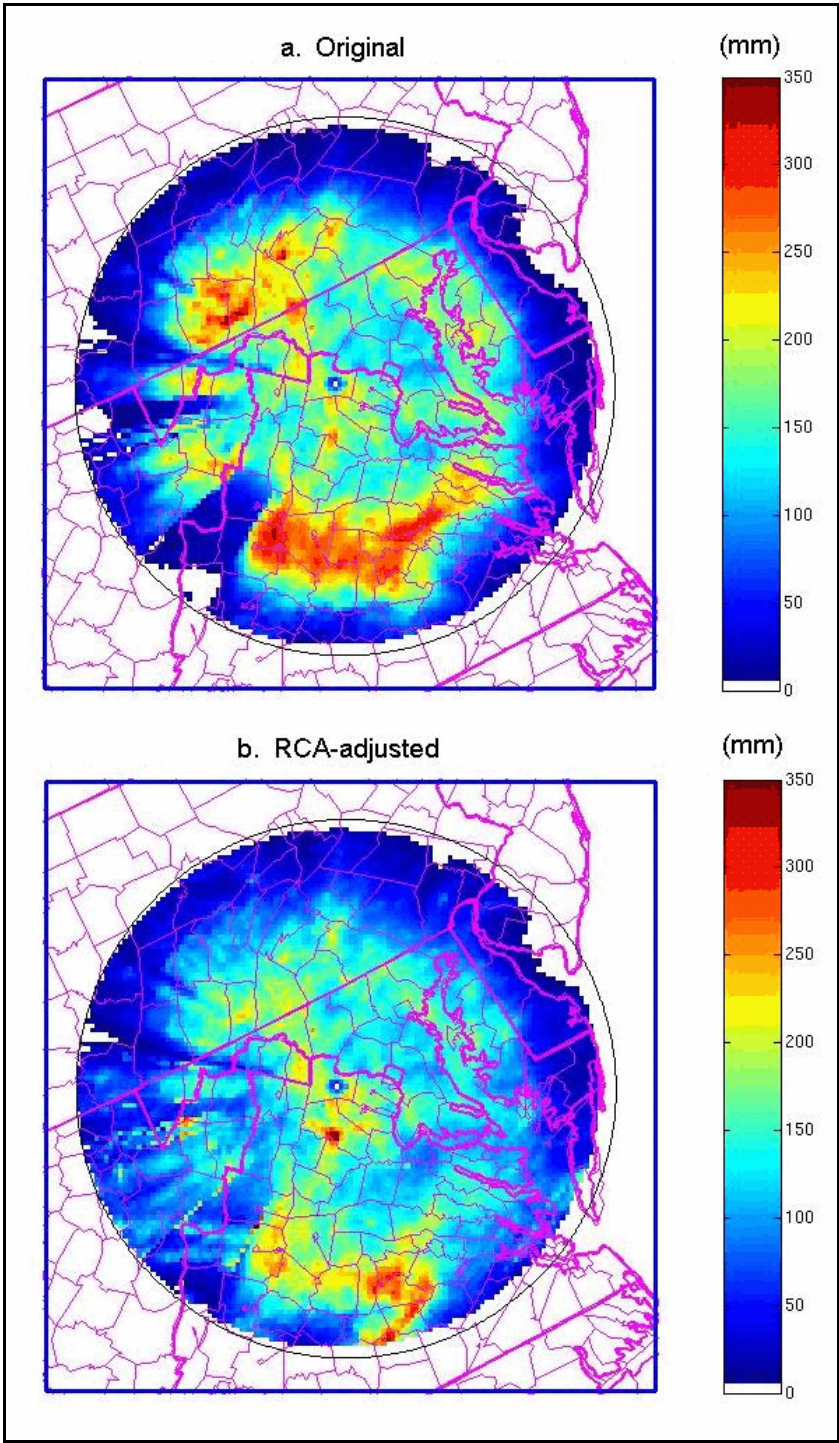


Figure 3. As in Fig. 1a,b, but for May 2003.

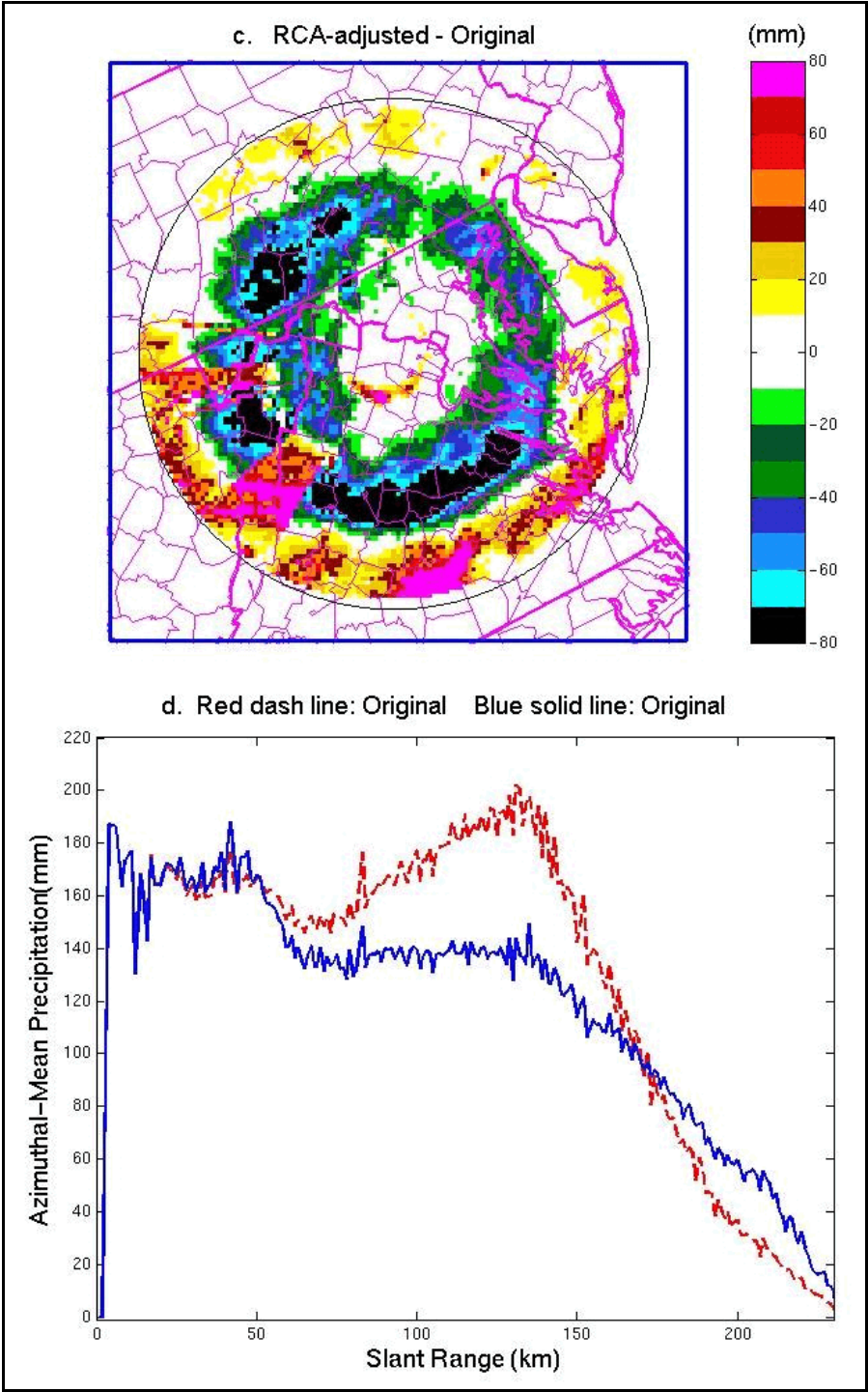


Figure 3(continued). As in Fig. 1c,d, but for May 2003.

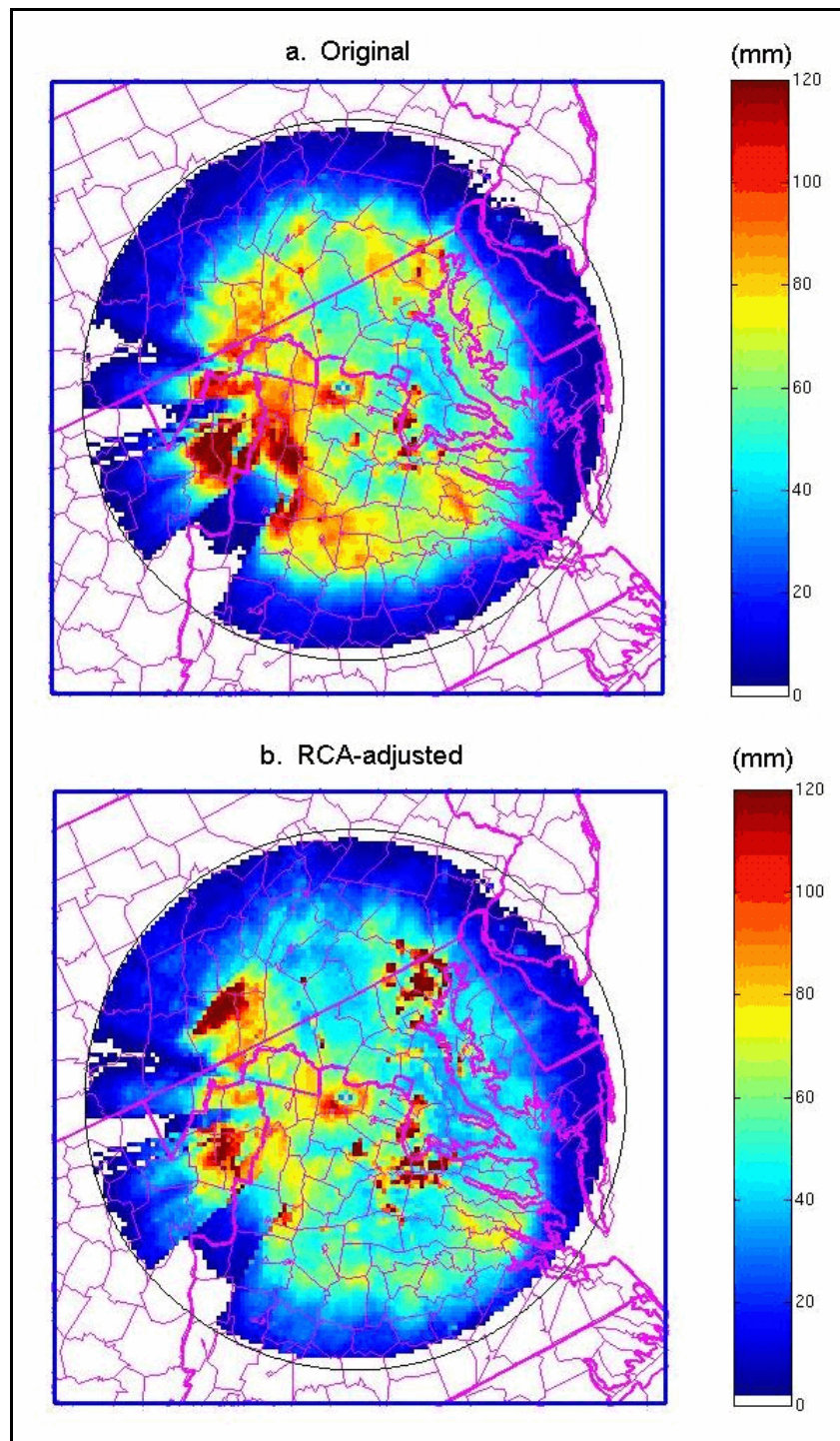


Figure 4. As in Fig. 1a,b, but using all data from April 2003.

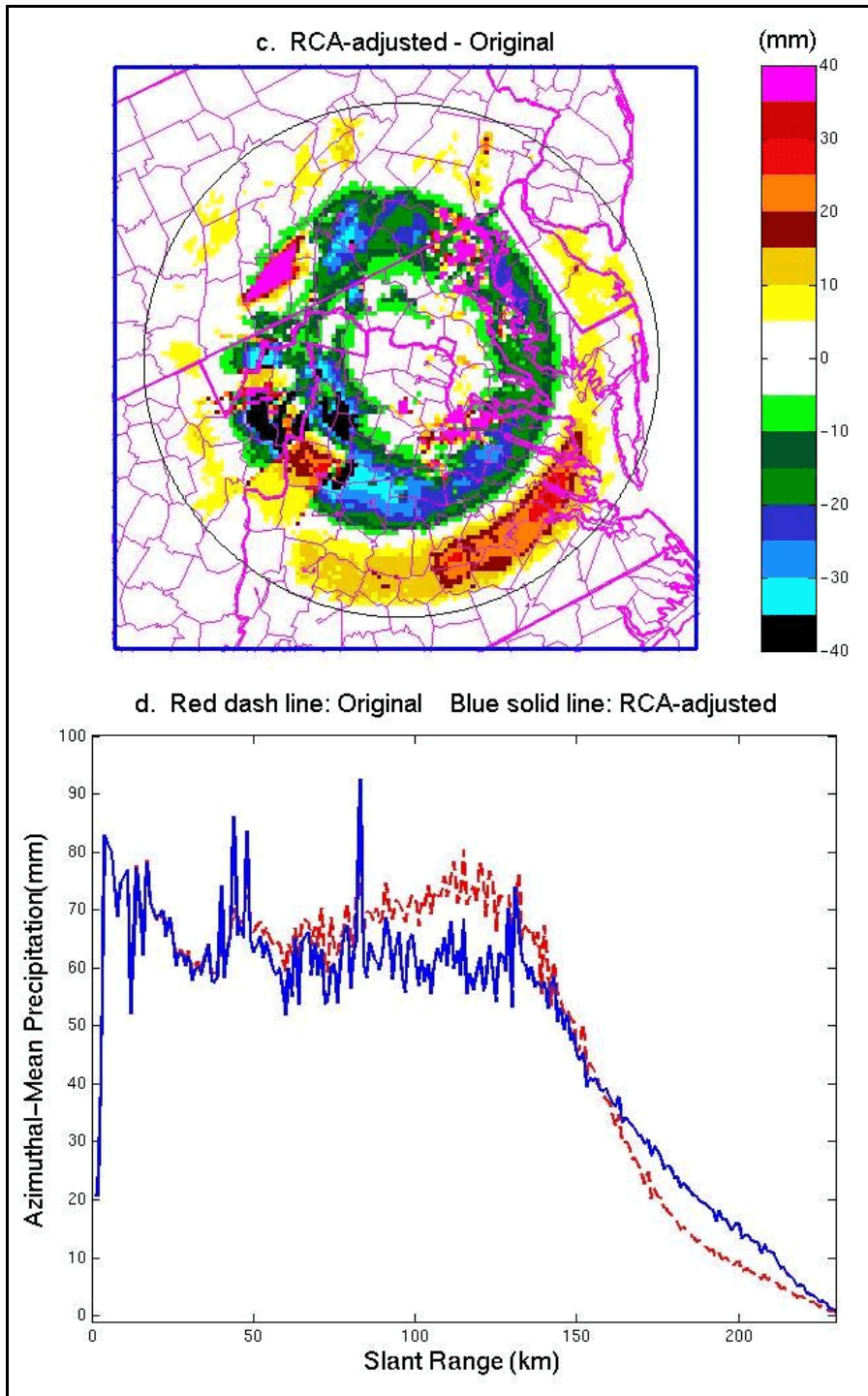


Figure 4(continued). As in Fig. 1c,d, but for all data in April 2003.

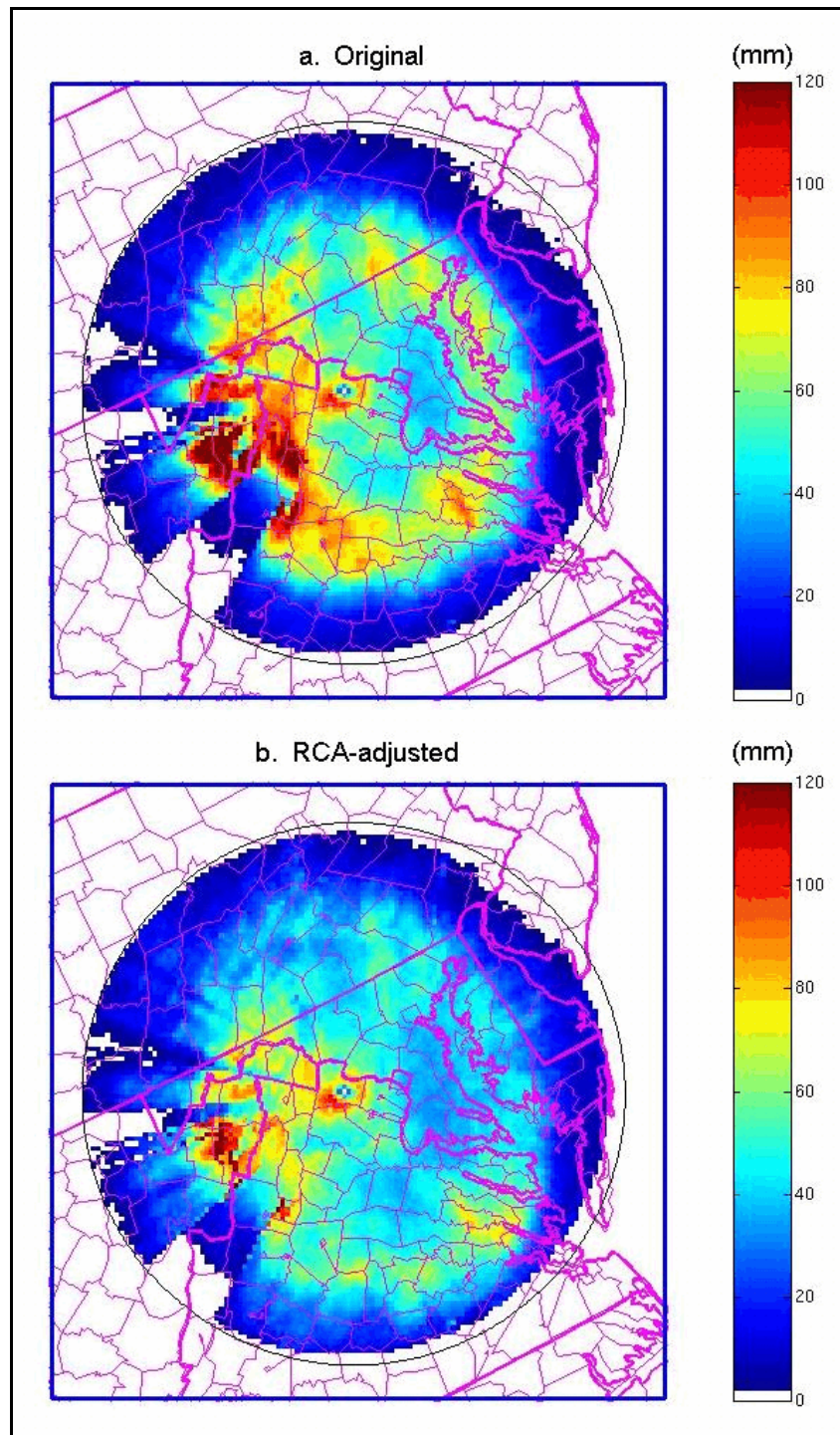


Figure 5. As in Fig. 1a,b, but for April 2003 data excluding 2 days with serious AP contamination.

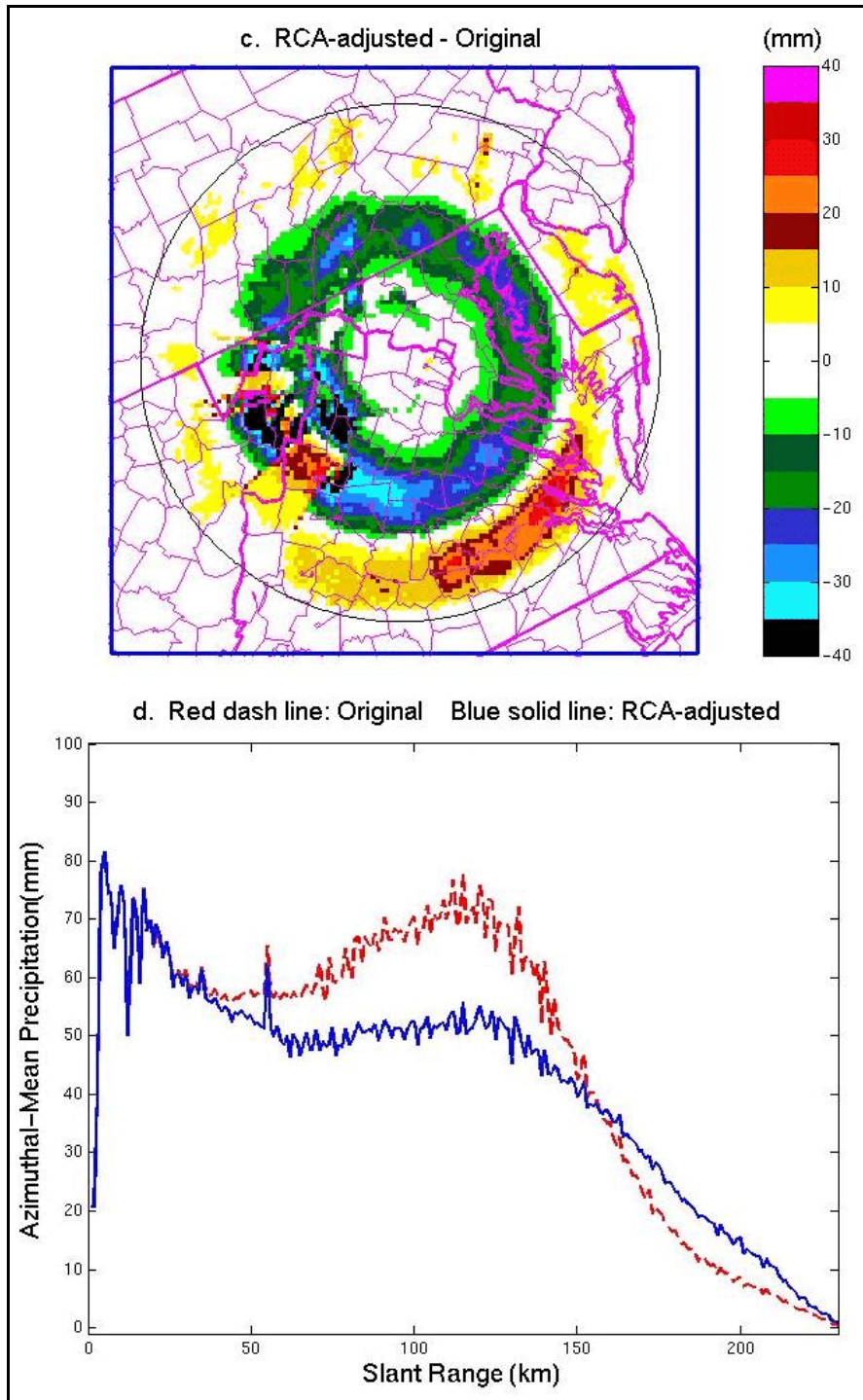


Figure 5(continued). As in Fig. 1c,d, but for April 2003 data excluding 2 days with serious AP contamination.

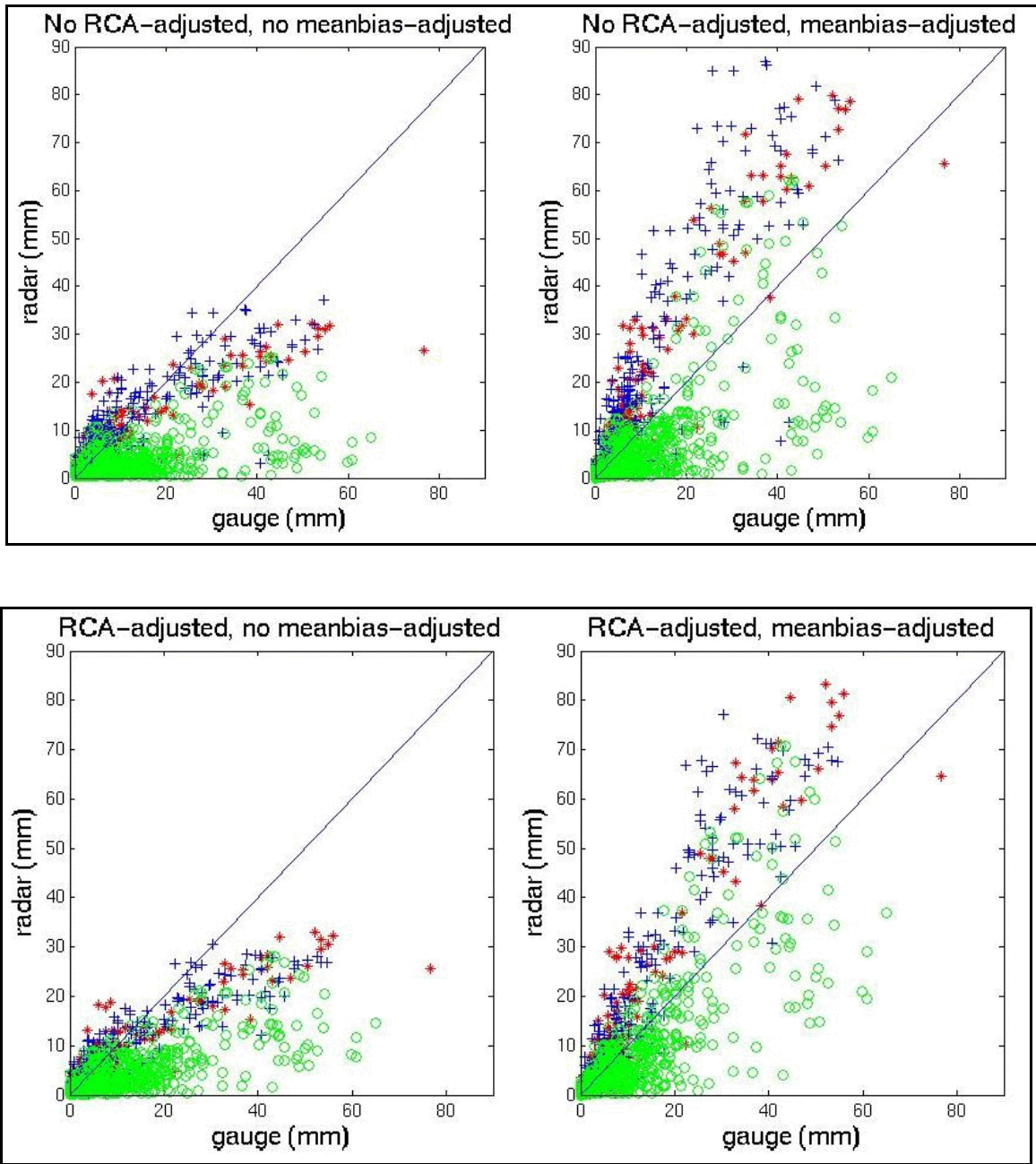


Figure 6. Scatter plots of 24-h precipitation, gauge vs. radar, in February 2003 (blue crosses from near-range; red stars from mid-range; green circles from far-range).

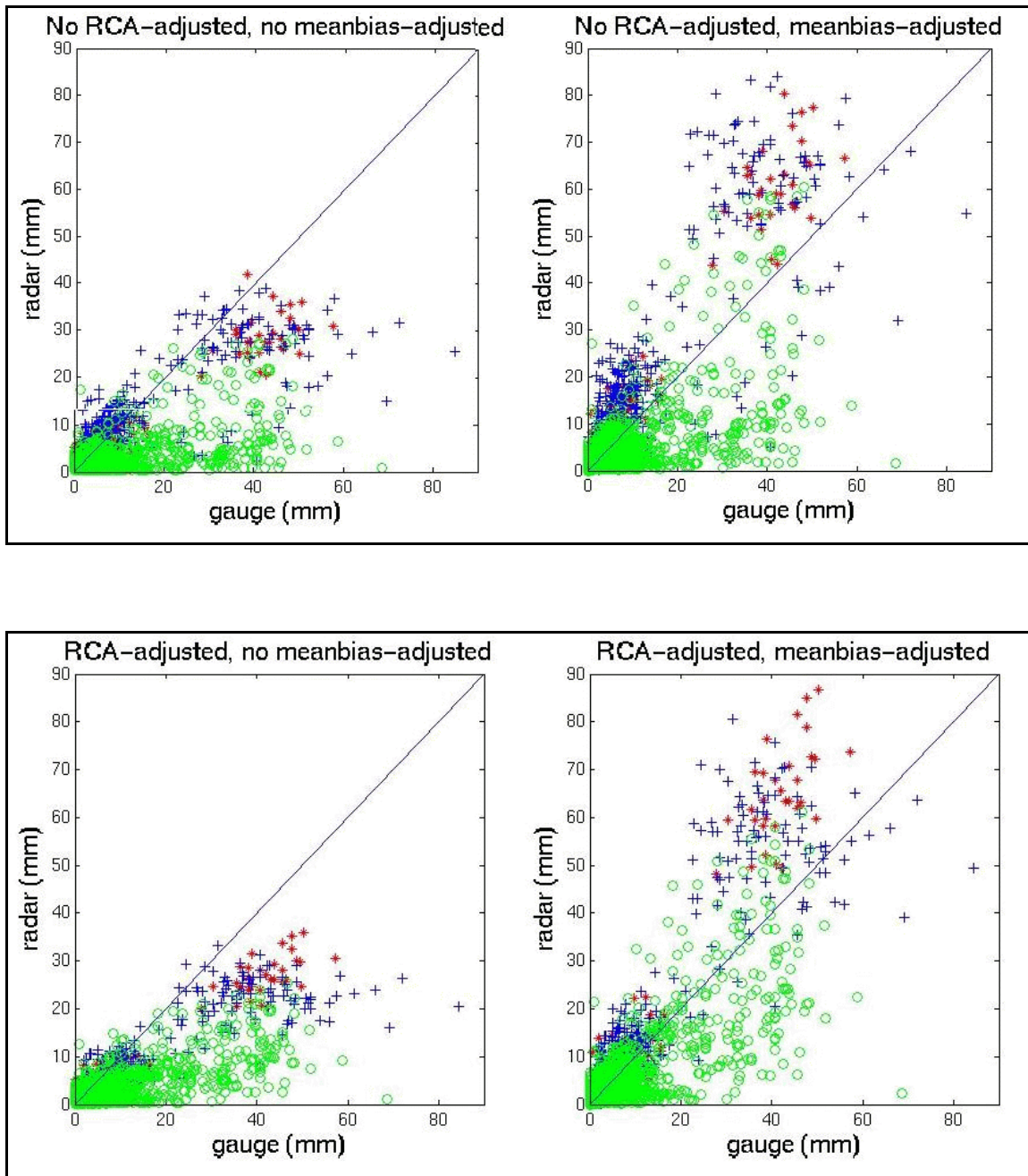


Figure 7. As in Fig. 6, except for March 2003.

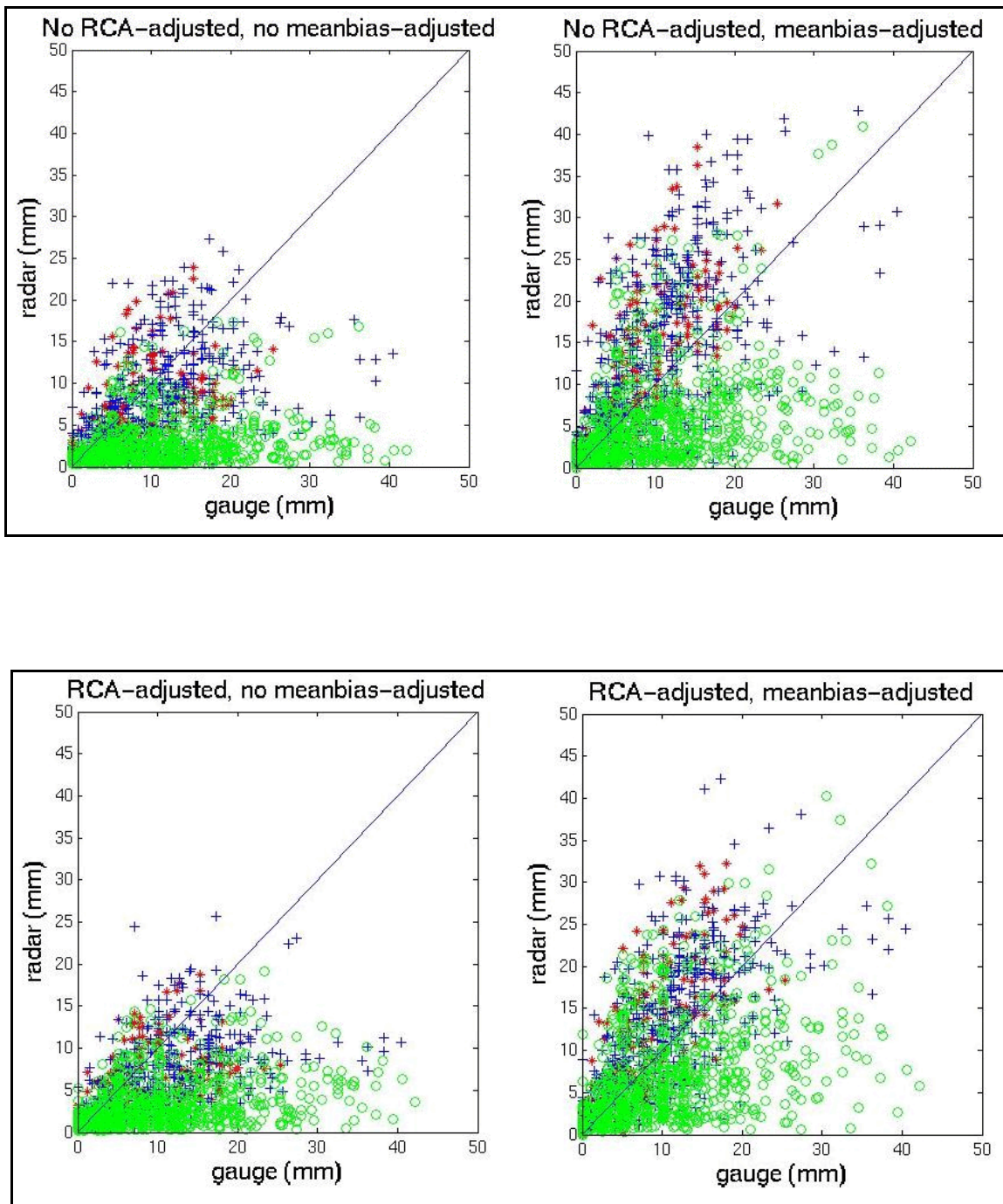


Figure 8. As in Fig. 6, but for April 2003.

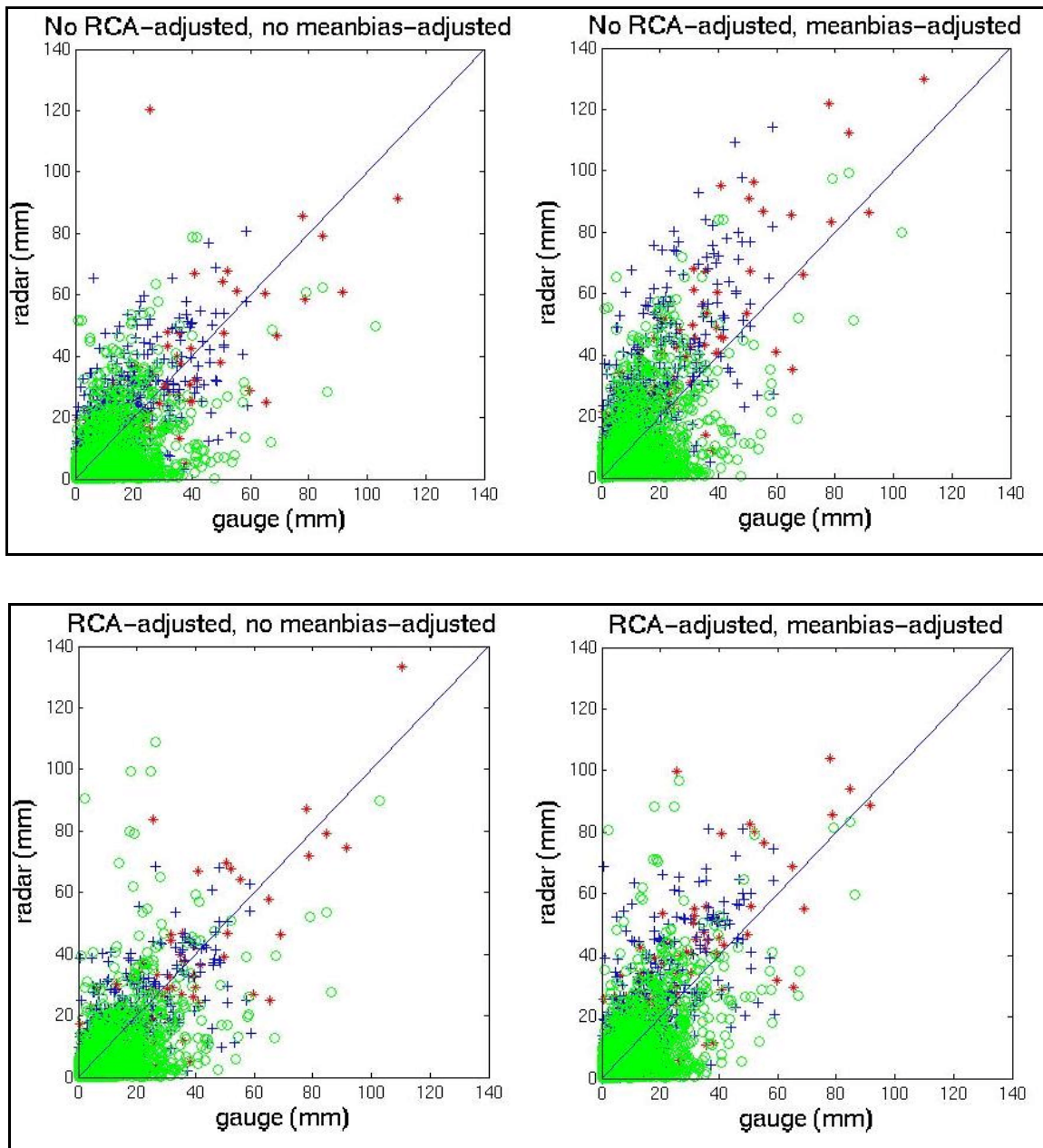


Figure 9. As in Fig. 6, but for May 2003.